

Cool Roof and Green Roof Adoption in a Metropolitan Area: Climate Impacts during Summer and Winter

Cheng He, Junri Zhao, Yan Zhang, Li He, Youru Yao, Weichun Ma,* and Patrick L. Kinney*



Cite This: *Environ. Sci. Technol.* 2020, 54, 10831–10839



Read Online

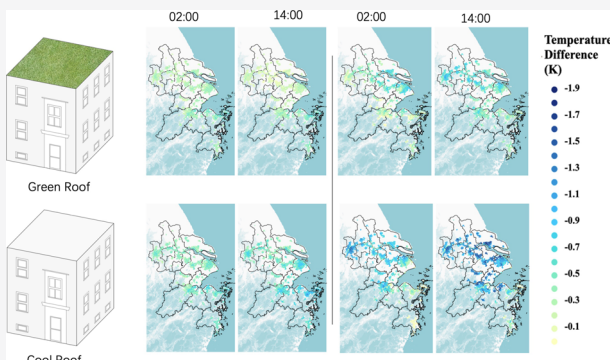
ACCESS |

Metrics & More

Article Recommendations

Supporting Information

ABSTRACT: This study, for the first time, estimates the climate impacts of adopting green roofs and cool roofs on the seasonal urban climate of 16 cities that comprise the Yangtze River Delta metropolitan. We use a suite of regional climate simulation to compare the local climate impacts of the implementation of different roof strategies in summer and winter. The results indicate that in summer, the 2 m surface temperature reduced significantly when these two roof strategies are adopted, with peak reductions of 0.74 and 1.19 K for green roofs and cool roofs, respectively. The cooling impact of cool roofs is more effective than that of green roofs under the scenarios assumed in this study. Besides, rooted in the different mechanisms influencing urban heat flux, significant indirect effects were also observed: adopting cool roofs leads to a decreased precipitation in summer and an apparent reduction in wintertime temperatures in the urban area. Although cool roofs can be an effective way to reduce high temperatures during the summer, green roofs have fewer adverse impacts on other climate conditions. These results underline the need for comprehensive climate change policies that incorporate place-based solutions and extend beyond the nearly exclusive focus on summertime cooling.



1. INTRODUCTION

The urban heat island (UHI) phenomenon is induced by urbanization and refers to cities being warmer than surrounding areas.^{1,2} High temperatures in urban areas exacerbate public health impacts,^{3,4} lead to higher energy consumption from air conditioner use,⁵ and potentially promote higher levels of air pollutants.^{6,7} In contrast, the UHI phenomenon can also have some benefits, such as increasing winter temperatures,⁸ which would lessen the heating demand and reduce the adverse effects of extreme cold.

Several aspects of urbanization aggravate the UHI effect, including anthropogenic heat (AH) released from the daily activities of residents and industrial production⁹ and the widespread use of materials with high heat capacities, which increase the urban heat storage of solar energy.¹⁰ Some consequences of urbanization could also mitigate urban warming; for example, increases in the vegetation cover in urban areas can influence evaporative cooling and shading of the ground surface.¹¹ Wind flows and vertical mixing are altered by green surface characteristics, with subsequent effects on temperature.¹² Together, these features have significant effects on the UHI patterns experienced in cities.

Many cities around the world are planning adaptation measures to lessen the negative impacts of urban warming, often with a focus on reducing local temperatures. Several mitigation strategies have been proposed in related studies.^{13,14} Among them, roof strategies, including green roofs and cool

roofs, are the most promising climate adaptation measures^{15–17} because roofs provide a large surface area for regulating the temperature in most cities. Improving the amount of green cover on roofs¹⁸ or increasing the albedo (i.e., reflectivity) of roofs to absorb less heat relative to standard roofs can cool the surrounding air.¹⁷ The cooling effect of these roof measures has been confirmed through observational and modeling studies in various regions across the world.^{19–21} Kusaka²² used the Weather Research and Forecasting (WRF) model to investigate the effects of green roofs and cool roofs on the urban climate of Chicago. Based on direct parameterizations of green and cool roofs, Li¹⁵ introduced a new urban parameterization model, the Princeton single-layer urban canopy model (UCM), coupled with the WRF model to assess changes in the surface UHI effect due to cool/green roofs. In some recent studies, more and more researchers have assessed the effectiveness of green/cool roofs via using the coupled WRF model with the single-layer UCM. For example, in Guangzhou, average urban midday temperature reductions

Received: June 1, 2020

Revised: August 4, 2020

Accepted: August 5, 2020

Published: August 5, 2020



of 1.2 °C on heat-wave days were induced by cool roofs.²³ In southern California, researchers found that summer urban air temperatures could be reduced by 0.9 K at 14:00 LST and by 0.5 K at 22:00 LST through the widespread adoption of cool roofs.²⁴ In Melbourne, the maximum surface UHI effect has been reduced during heat-wave days by 1–3.8 °C by increasing the fraction of green roofs from 30 to 90% and by 2.2–5.2 °C by increasing the albedo of cool roofs from 0.50 to 0.85.²¹ Thus, both roof types can reduce the summertime temperature effectively, while the mechanisms by which green roofs and cool roofs produce cooling impacts are different. Green roofs increase the evapotranspiration through the soil and plants on the roof; cool roofs increase the reflection of incoming solar short radiation by increasing the albedo of roof surfaces.¹⁵ In addition to cooling impacts, these roof measures may lead to the varied impacts on other climate conditions.

A few studies have investigated the influence of roof strategies on climate conditions other than summertime temperatures. For example, research in Athens has shown that adopting cool roofs induced a 0.5 °C temperature reduction in winter.²⁵ In Italy, researchers found that cool roofs reduced the maximum winter cooling by up to 1.2 °C.²⁶ These studies have not adequately determined the potential impacts of green/cool roofs on climate conditions other than high temperatures in summer. As such, the potential impact of green/cool roofs on urban climate conditions remains an open yet extremely critical question, particularly because the climate effect of green/cool roofs has shown to vary depending on the local background climate in cities.¹⁷

In this study, we used the advanced research version of the WRF regional climate model coupled with the UCM to investigate how the adoption of green roofs and cool roofs influences not only temperature but also other climate conditions in the Yangtze River Delta (YRD) urban agglomeration, which is the most urbanized area in China. Three questions are addressed in this paper: (a) How do different roof strategies affect urban temperatures? (b) How effective is the cooling from green and cool roofs during the summer in the YRD? (c) What potential climate impacts do green and cool roof strategies have beyond summertime cooling?

2. METHODOLOGY

2.1. WRF Modeling. In this study, we use the WRF model version 3.8.1 to investigate the potential influence of adding green roofs and raising the roof albedo on the urban climate in the YRD. The WRF model was jointly developed by the National Oceanic and Atmospheric Administration (NOAA), the National Center for Atmospheric Research (NCAR), and other researchers. It is a state-of-the-art, non-hydrostatic, fully compressible numerical weather prediction model with wide-ranging utility.^{16,17}

The WRF model provides several schemes that can be used to model the weathering process at a fine scale. We chose several schemes for modeling at the urban scale based on several related studies.^{16,23,24} Among these schemes, the physics scheme includes the longwave radiation scheme of the rapid radiative transfer model (RRTM),²⁷ shortwave radiation scheme of the Dudhia shortwave radiation,²⁸ and the microphysics scheme of Purdue Lin microphysics scheme.²⁹ The Noah land surface model³⁰ was used to model exchanges of energy, water, and other variables. More importantly, we incorporated WRF with the single-layer UCM

to model the surface-atmosphere process in urban areas. This model resolves the temperature variations at the top of the urban canopy, as it incorporates all factors of the urban canopy.¹⁷ Thus, it has the potential to assess the impacts of different roof strategies on urban climates. Specifically, in the UCM, the urban canopy consists of a long street bounded by buildings with a uniform width. When the downward shortwave solar radiation is not absorbed by urban canopy, it will be reflected out of the canopy as outgoing shortwave radiation.²⁴ In this process, the UCM calculates the latent heat flux and sensible heat flux changes over the rooftop, which takes different roof properties into consideration. That is, the changes in heat flux induced by cool roofs and green roofs were calculated here. Notably, these roof properties can be modified only in the urban fraction of each grid cell; it is not used in other parts of the modeling process in the WRF calculations.

Some of the essential parameterizations that we chose for the WRF model are listed in Table 1 in detail, and the other input parameters related to the urban attributes in the UCM are listed in Table 2 based on related research studies.

Table 1. Physics Options for the WRF Model

items	options	reference
microphysics	Purdue Lin microphysics scheme	Lin et al., ³¹
longwave radiation	RRTM scheme	Mlawer et al., ³²
shortwave radiation	Goddard scheme	Kim and Wang ³³
land surface	Noah land surface model	Chen and Dudhia ³⁴
surface layer	Eta similarity	Janjic ³⁵
cumulus parameterization	Grell 3-D	Grell and Dévenyi ³⁶

2.2. Land-Cover Information in the Model Setting.

Studies have demonstrated that replacing the default representation of land surface information with satellite-based characteristics improves the performance of the coupled WRF/UCM model.^{24,40} To improve the accuracy of the model, we used the MODIS monthly data on the green vegetation fraction (GVF), leaf area index (LAI), and albedo to modify the corresponding values in our WRF/UCM modeling system. For this purpose, we used ArcGIS and Python to regrid and incorporate MODIS data in the WRF/UCM framework, thereby improving the GVF and LAI values in the study area.

More importantly, we used urban land use data from the China land-use and land-cover change data (CNLUCC), which can be obtained from the Resource and Environment Data Cloud Platform of the Chinese Academy of Sciences (<http://www.resdc.cn/>), to depict the urban fraction of grid cells. There are three urban land use types in the WRF/UCM model including low-intensity residential, high-intensity residential, and commercial/industrial centers, with different intensities of AH emissions. To divide all urban areas into these three types, we computed the AH emissions in the 16 cities and further divided all urban areas into three types according to the level of AH emissions. In practical terms, based on preset values in the UCM model and the results from other related research,⁴¹ we regard urban area with AH emission higher than 60 W/m² as the commercial/industrial center, with AH emission ranging from 20 to 60 W/m² as high-intensity residential, and with AH emission lower than 20 W/m² as low-intensity residential. The spatial pattern of the three

Table 2. Input Parameters of the UCM Model (Based on: Xie et al.^{37,38} and Stewart et al. 2014³⁹)

items	commercial/industrial center	high-intensity residential	low-intensity residential	unit
mean building height	20	5	3	m
canyon height-to-width ratio	2	0.5	0.25	
facet heat capacity ^a	1.8, 1.8, 1.8	1.5, 2.1, 1.8	1.5, 2.1, 1.8	MJ m ⁻³ K ⁻¹
facet thermal conductivity ^a	1.2, 1.1, 0.8	1.1, 1.3, 0.8	1.0, 1.2, 0.8	W m ⁻¹ K ⁻¹

^aThe number for this part is in this order: roofs, walls, roads.

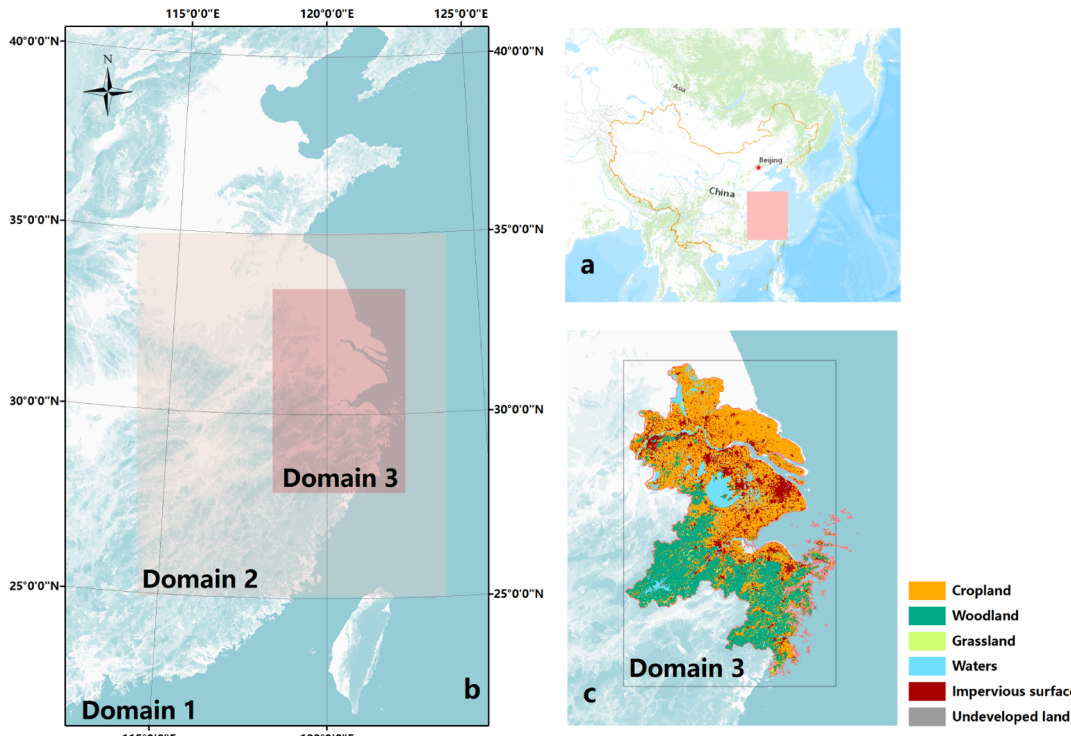


Figure 1. Nested domains used in the WRF/UCM model in this study. Location of the study area in China (a). Resolutions of the three studied domains are 27, 9, and 3 km, respectively (b). Spatial distribution of different types of land use in YRD agglomerations (c).

types of urban area is depicted in Figure S1. For more information on the calculation methods and the results for all types of AH emissions, see our other study in detail.⁴²

2.3. Simulation Domain. We chose the YRD metropolitan as the simulation domain for three reasons: (1) The YRD metropolitan area is the largest urban agglomeration in China and its economic center. It has experienced a progressive urbanization process. Notable urban warming trends in the past several years constitute the most severe current warming conditions.⁴³ Obvious UHI effects in this area highlight the need for urban planning strategies. (2) The Chinese government recently introduced a series of policies to promote economic integration for these areas; future human activities are expected to intensify the warming impacts. It is necessary to conduct related research on region-based planning and design strategies to reduce the negative impacts of urban warming. (3) Most modeling studies on the effects of urban warming and the mitigation measures have been focused at a single city scale. Research covering multiple cities is limited. A total of 16 cities with different urban sizes and socioeconomic backgrounds but similar climatic conditions comprise the YRD metropolitan area, as shown in Figure 1. Multiple-city studies can yield more general conclusions for the cities with similar climatic conditions, although there would be some differences in the actual building geometry and physical properties

between these cities, which would affect the UCM performance. We still will be able to reflect some different inner structures and the building features over 16 cities by using spatial patterns of AH emission because the varying magnitude of AH emission represents different population density and urban features.⁴⁴

For these purposes, all urban areas in the YRD metropolitan area are covered in our analysis. Three nested domains with resolutions of 27, 9, and 3 km were simulated. As shown in Figure 1, the outer domain (d1) covers eastern China, the middle domain (d2) covers the south-eastern part of China, and the inner domain (d3) covers the entire YRD metropolitan area, which includes 16 cities. According to the settings of the WRF model, the inner domain uses values from the adjacent weather background of the outer domain as boundary conditions, and the outermost domain (d1) uses the global operational final (FNL) data as boundary conditions. The FNL data have a temporal resolution of 6 h, with a spatial resolution of $1^\circ \times 1^\circ$.

2.4. Simulation Design with the WRF/UCM Model. The evaluation of potential climate impacts from two roof adaptations is based on three scenarios. First one is the BASELINE scenario, the albedo of roofs is set according to real situations. Based on an observational research in China,⁴⁵ we set the building roof albedos at 0.12 across the urban areas.

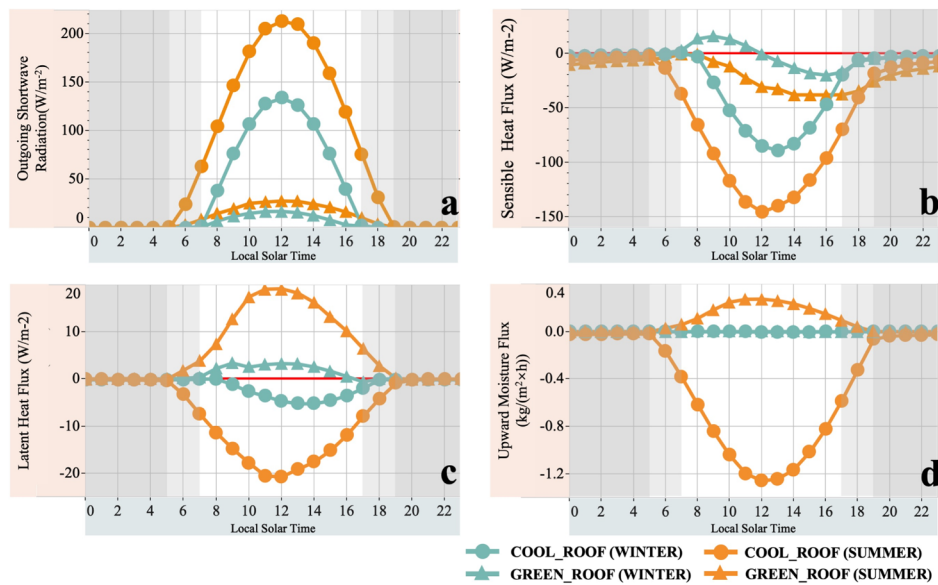


Figure 2. Diurnal differences of outgoing shortwave radiation (a), sensible heat flux (b), latent heat flux (c), and upward moisture flux (d) between two roof scenarios and BASELINE scenario in YRD. All values are seasonal average of the urban grids in local solar time. The dark gray area represents the night in summer and winter, and the light gray area represents the additional night in winter.

The GREEN_ROOF scenario assumes that 80% of the roofs in urban areas are vegetation-covered roofs with adequate water availability on roofs. In the UCM setting, green roofs consist of four different layers, including a grassland layer, a loam soil layer for grassland, a growing medium layer, and a common concrete roof layer, and the default soil moisture of the green roof layer is $0.20 \text{ m}^3 \text{ m}^{-3}$. The COOL_ROOF scenario assumes uniform application of a high albedo coating with 0.65 albedo on all roofs in the urban areas. The coverage of the green roofs and the albedo of the cool roofs is based on active policies and actual observations, respectively. For green roofs, many cities in the YRD have introduced related policies to encourage the adoption of green roofs. For example, the Shanghai Municipal Greening Regulations require all newly built public buildings to adopt green roofs, and the total coverage of green roofs is required to be not less than 50%. In Hangzhou, over 420,000 square meters of green roofs have been added in urban areas since 2010. For cool roofs, the albedo value of cool roofs represents the average albedo of currently available and used white roofing products in China based on actual observations.⁴⁵ Our goal of applying an albedo of 0.65 in the COOL_ROOF and 80% adoption rate in the GREEN_ROOF is to demonstrate the potential impact of a feasible near-future scenario of the upper bound of climate effects based on existing policies and status quo.

Simulations were conducted in winter (from last December 1st to February 28th) and summer (from June 1st to August 31st) in 2016. All simulations were divided into several parts, each part was performed for 16 days, and the first 24 h were discounted as “spin-up day”, considering the intrinsic uncertainties in the initial part of the simulation. Tables S1, S2 and S3 show a statistical comparison of the BASELINE scenario results and meteorological observation data from 16 stations located in 16 cities in both winter and summer seasons. The spatial distribution of 16 weather observation stations is shown in Figure S2. Overall, these results demonstrate the ability of the BASELINE scenario to capture

regional variations in the temperature, relative humidity, and wind speed across the YRD.

3. RESULTS AND DISCUSSION

3.1. Diurnal Variation of Reflected Solar Radiation.

Based on related research,²⁴ we defined the outgoing shortwave radiation as the incoming shortwave radiation multiplied by the grid cell albedo. Figure 2a shows the diurnal variation of outgoing shortwave radiation changes in the urban area resulting from the adaptation of green/cool roofs. The values under three scenarios are shown in Figure S3. As shown in Figures 2a and S3a, the increase in the outgoing shortwave radiation induced by two roof strategies reaches its maximum value when the incoming shortwave radiation peaks around the solar noon. In comparison, the increase in the outgoing shortwave radiation under the COOL_ROOF scenario is significantly greater than that under the GREEN_ROOF scenario. That is, the urban area albedo changes under the COOL_ROOF scenario lead to higher increases in the daily cumulative reflected solar radiation in both summer and winter.

3.2. Diurnal Variation of Urban Heat Flux. Figure 2b,c depicts changes in the urban heat flux induced by green/cool roofs in two seasons. The specific values of the urban heat flux under three scenarios, including BASELINE, GREEN_ROOF, and COOL_ROOF scenarios, are shown in Figure S3b,c.

As shown in Figures 2b and S3b, adopting cool roofs can constantly and significantly reduce the sensible heat flux in two seasons. These reductions are related to the great increase in the outgoing shortwave radiation induced by cool roofs, which reduces the total energy passing into the urban canopy. The diurnal changes are broadly similar to the change pattern of the outgoing shortwave radiation; they both reach their maximum around solar noon. In terms of the latent heat flux, as shown in Figure 2c, it is interesting to observe that adopting high albedo roofs will still reduce the latent heat flux, although there are no evapotranspiration changes on the cool roofs. This is due to the reduction of the total energy, especially in summer.

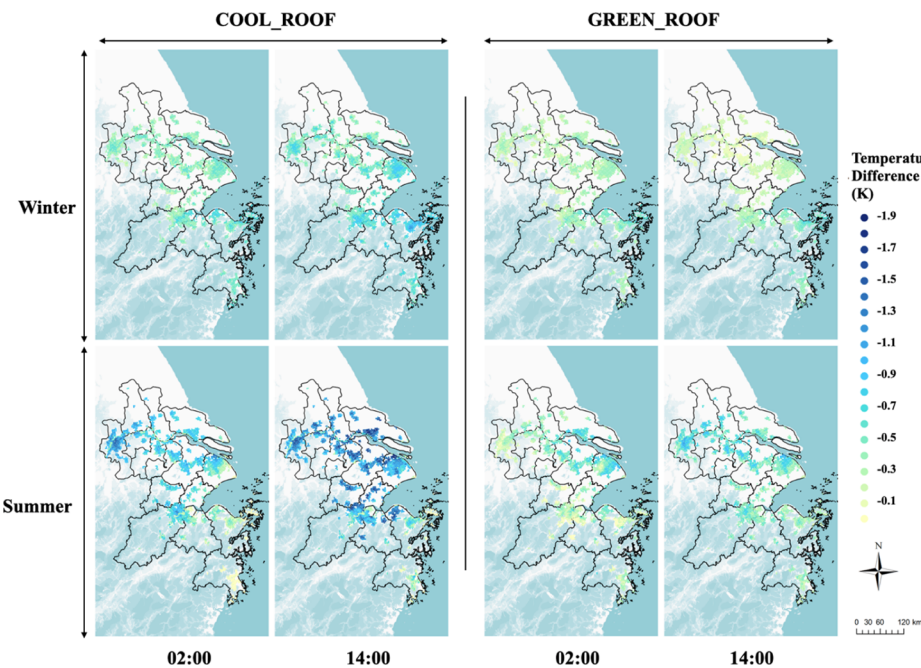


Figure 3. Spatial differences between the two roof strategy scenarios and the BASELINE scenario for the 2 m temperature. The values represent the averages at 02:00 LST and 14:00 LST for winter and summer within 16 cities. Differences that are nonsignificant under the 95% confidence level are masked out.

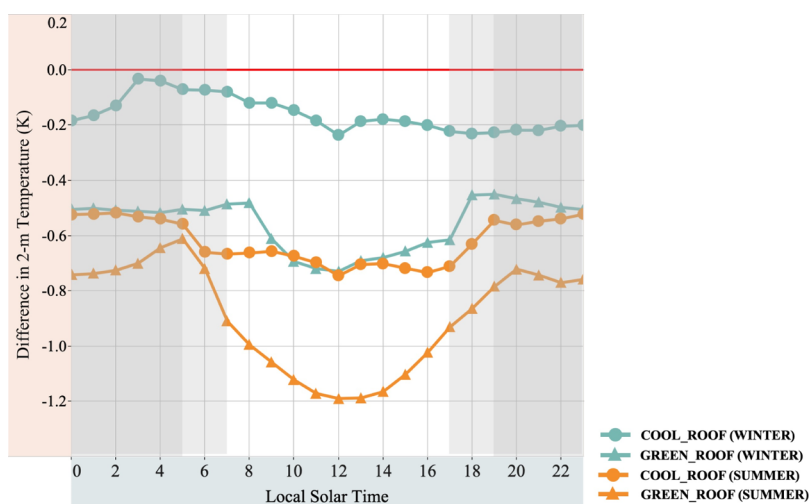


Figure 4. Diurnal differences of 2 m temperature in YRD between two roof scenarios and the BASELINE scenario. All values are the seasonal average of the urban grids in local solar time. The dark gray area represents the night in summer and winter, and the light gray area represents the additional night in winter.

Compared with cool roofs, green roofs increase the latent heat flux into the atmosphere more significantly via stronger evapotranspiration in summer. However, it changed the sensible heat slightly because of the limited changes in the total reflected radiation. On winter mornings, when the amount of outgoing shortwave radiation induced by green roofs is lower, it is interesting to observe that the stronger evapotranspiration induced by green roofs increases the latent heat flux and the sensible heat flux at the same time. When the amount of outgoing shortwave radiation increases as the hours passed into noon, the sensible heat flux tends to decrease. Because of the comprehensive changes in the latent heat flux and other atmospheric conditions, the sensible heat flux reduction induced by green roofs obtains its maximum value

after solar noon, which is later than that happened under COOL_ROOF.

Besides, Figures 2d and S3d depict the impacts of green and cool roof strategies on the upward moisture flux at the urban surface, which is an indirect effect related to changes in the heat flux. As shown in Figure 2d, there is no significant difference during winter, when the land-atmosphere coupling strength is weaker because of the lower background temperature and the small amount of water vapor and also because the baseline value of upward moisture flux in winter is deficient, as shown in Figure S3d. Hence, we only focus on the results in summer. As seen from Figure 2d, green roofs can significantly increase the daytime upward moisture flux. This can be explained by the significant increases of latent heat

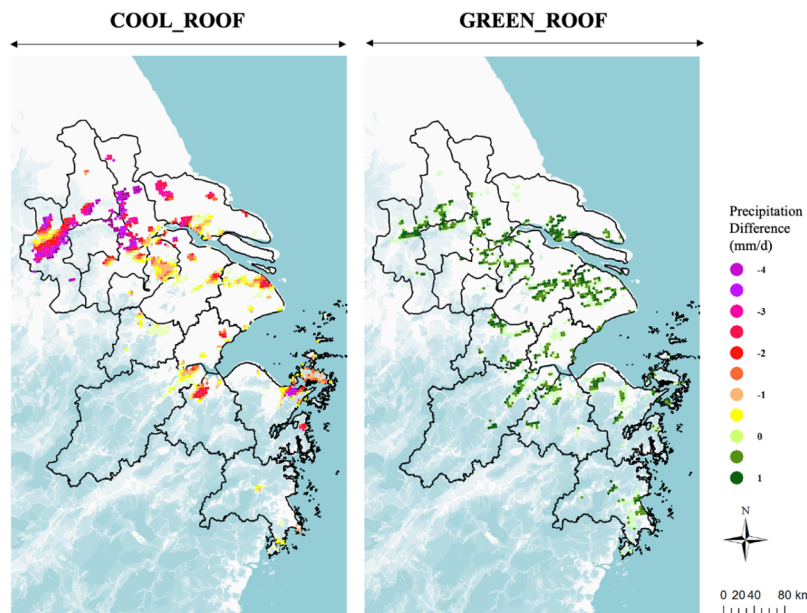


Figure 5. Spatial differences between the two roof strategy scenarios and the BASELINE scenario for surface precipitation. The values represent averages for summer. Differences that are nonsignificant under the 95% confidence level are masked out.

under the GREEN_ROOF scenario. In contrast, the upward moisture flux decreased because of the adoption of cool roofs. This is caused by the reduction of sensible heat under COOL_ROOF that weakens the energy to transport moisture upward. Besides, the more immediate reason is that the reduction of latent heat flux under COOL_ROOF will lessen the upward moisture flux directly. When the total heat flux over the urban surface is reduced by cool roofs, the internal moisture that is supposed to climb with air flows from the surface increases less rapidly. This means that at a given water vapor total, the water vapor content in the upper atmosphere decreases over the urban area. It will affect precipitation in the city.

3.3. Spatial Variation in the 2 m Temperature. Figure 3 depicts the impact of green roof and cool roof strategies on the 2 m temperature over study area. To completely depict the temperature impact in the entire urban area, in addition to the grids dominated by the urban area, we selected all the grids within the urban boundary of 16 cities, including the urban core and suburb area and excluding rural and natural areas of each city, by using night-time light data and population distribution data, as we have discussed elsewhere.⁴²

In summer, the results show a similar cooling pattern for green and cool roofs, whereas the cooling impact induced by cool roofs is stronger than that induced by green roofs over most urban areas. Temporally, daytime cooling [14:00 local solar time (LST)] is stronger than night-time cooling (02:00 LST). Spatially, the total reductions in the 2 m temperature are mainly due to reductions in the urban core; however, changes in the suburbs are also observed, as shown in Figure 3. This is to be expected downwind of the city where urban cooling could lead to slight rural cooling because of reduced heat advection.

In winter, only cool roofs induced an obvious cooling impact at two different times. The reason for these phenomena is discussed in Section 3.4 in detail.

3.4. Diurnal Variation of the 2 m Temperature. The diurnal changes in the 2 m temperature of the two roof

strategies are illustrated in Figure 4. As seen from this figure, the two roof measures lead to widely different diurnal temperature cycles in the two seasons.

For green roofs, we only focused on the differences in summer, considering that the reductions in winter are limited. As shown in Figure 4, the green roof strategy can significantly reduce the daytime temperature, but the cooling impacts during the night-time are moderate. This can be explained by two facts: (1) green roofs induce significant increases in evapotranspiration during daytime but have a weaker impact during night-time, considering the energy limitation of night-time evapotranspiration on total heat balance. (2) The green roof strategy induces a significant cooling effect during the daytime, which can probably last into the night because of reduced total heat storage in the urban canopy. In addition, the performance of green roofs described here is closely linked to changes in the latent heat flux, so the maximum reduction occurs nearly at the same time when the background temperature reaches its maximum in the early afternoon.

For cool roofs, in summer, it also induces a stronger temperature reduction, and the diurnal pattern of reduction is broadly similar to that of green roofs. The peak temperature reduction of 1.19 K occurs at solar noon, with the reductions of the sensible heat peaks, as shown in Figure 4. In addition, cool roofs also present a lower impact on the night-time temperature than on the daytime temperature, and this difference between day and night induced by cool roofs is even higher than that induced by green roofs. This is related to the absence of incoming solar radiation during the night: albedo no longer plays a key role in the city-scale energy balance. Nevertheless, cool roofs still maintain some influence on the night-time urban temperature, suggesting that the daytime cooling effect can be extended into the night-time, which is similar to green roofs. In contrast, in winter, cool roofs will still significantly reduce the temperature, and the diurnal pattern of the winter temperature is similar to the changes in summer, which reach the maximum at solar noon and have a certain impact throughout the day. These results confirmed

that the reason why cool roofs induce a temperature change is different from that of green roofs and is more strongly related to the reduction of the sensible as well as latent heat rather than the latent heat increase for green roofs.

A comparison of the green roof and cool roof results suggests that in summer, the cooling effect of cool roofs, with an albedo value of 0.65, is higher than that of green roofs. This result is slightly different from the studies of Li¹⁵ and Gaffin,⁴⁶ which suggested that the albedo required on nongreen roofs to reproduce the cooling impact observed on green roofs is in the range from 0.70 to 0.85 for cities located in Northeast Megaregion of the United States. We think this is because the YRD area is located in the subtropical climate zone, where the shortwave radiation in summer is higher than that of cities located in the Northeast Megaregion of the United States. Besides, in winter, the fact that the cool roof strategy still has a certain influence on the wintertime temperature confirmed that these two different roof strategies would induce significantly different impacts on the winter temperature.

3.5. Spatial Variation in Precipitation. Figure 5 depicts the city-scale impact of the green roof and cool roof mitigation strategies on the summertime precipitation. It should be mentioned that there is no significant difference produced in winter, given that the YRD area is located with a monsoon climate, where precipitation is concentrated in summer; thus, we focus on only the results averaged over the summer.

As seen from Figure 5, adopting green roofs can slightly increase the precipitation over urban areas. This result can be explained by the significant increase in upward moisture flux induced by green roofs. In contrast, cool roofs reduce the summertime precipitation in the urban proportion of the domain because the higher albedo of cool roofs increases the outgoing shortwave radiation, leading to less latent heat flux and upward moisture flux. This is an interesting indirect effect related to the changes in temperature over the urban area, which is consistent with Zahra,⁴⁷ who showed that adopting cool roofs in Montreal also reduced precipitation at the local scale.

Overall, cool roofs reduced urban precipitation by 6.7%, while the green roof increased the total by 1.7%, compared to the BASELINE. Although the changes of the total proportion are relatively small, it is expected to have implications for water demand and scarcity for human from stream flow and aquatic ecosystems, as the related study pointed out.⁴⁸

3.6. Research and Policy Implications. Using a suite of cross-season regional climate simulations, we provide the first assessment of the urban climate impacts of green roofs and cool roofs across 16 cities in the YRD area. Our results suggest although these two roof measures resulted in generally similar cooling patterns in summer, rooted in the different mechanisms affecting the urban heat flux, some different indirect effects were observed. First, uniformly adopting cool roofs will reduce the summertime precipitation within urban areas. The simulated decrease in precipitation is expected to have implications for water demand and aquatic ecosystems within urban systems. Second, the rejection of solar shortwave radiation by cool roofs significantly reduces wintertime urban temperatures, which may increase the electricity demand for indoor heating.¹⁷ There is little doubt that these indirect effects induced by cool roofs will negatively affect urban environments. Policies should consider multiscale environmental elements rather than focusing on one-purpose-fits-all policies.

This study also has some limitations. First, the impact of the two roof strategies is expected to vary with the background climate conditions and the feature of the built-up area, such as the concentration of shortwave radiation and precipitation in different seasons and the ratio of the roof area in the urban region. The results are thus quantitatively representative of climate and built-up area features in the eastern coastal region of China or in regions with similar climate and built-up area features. The climate impacts of these roof strategies for other regions would be different. For instance, an observation experiment in Italy suggests that the cool roof is an appropriate solution to improve summer energy performances, which is worth-enough to offset the negative impact during winter.⁴⁹

Second, we emphasize that the climate impacts of green roofs and cool roofs studied here are specific for a common type of green roof with a coverage of 80% and cool roof with an albedo of 0.65. For the cool roof, when the albedo of the cool roof is changed, the performance will also be modified, as related research has indicated.¹⁵ For the green roof, more factors can affect the performance as the related observation experiment pointed out,⁵⁰ such as vegetation species, soil moisture, and irrigation. In addition, because of the single layer setting in the WRF/UCM model, the overall impact of the green roof is not fully captured.¹⁵ However, these features will not influence some key findings from this study, such as the unexpected impact of cool roofs on wintertime temperature, the potential influence of cool roofs on precipitation during the summertime, and the seasonal characteristics of green roofs.

Third, different roof strategies will also affect other urban environments, which is beyond the scope of this study but worth discussing. One is the air quality, especially the concentration of particulate matter, which would be affected as the weather background altered under the adaptation of different roof strategies.⁵¹ Besides, the indoor temperature would also be affected, especially by the green roofs. When the soil layer was considered as the bottom of the green roof, it functioned as a “cooling source” that absorbed heat from the upside and downside to cool the indoor temperature.⁵²

Finally, we should also consider the economic cost. A study in the United States suggests that relative to the cool roof, the installation and maintenance costs of the green roof would be higher.⁵³

ASSOCIATED CONTENT

Supporting Information

The Supporting Information is available free of charge at <https://pubs.acs.org/doi/10.1021/acs.est.0c03536>.

Spatial pattern of the three types of urban area; 16 weather stations that we selected in this study for validating our simulation results; diurnal variation of outgoing shortwave radiation, sensible heat flux, latent heat flux, and upward moisture flux in YRD under three scenarios; and statistical comparisons between the “baseline” scenario results and meteorological observation data for 2 m temperature, relative humidity, and wind speed ([PDF](#))

AUTHOR INFORMATION

Corresponding Authors

Weichun Ma — Department of Environment Science and Engineering and Big Data Institute for Carbon Emission and Environmental Pollution, Fudan University, Shanghai 200438,

China; Shanghai Institute of Eco-Chongming (SIEC), Shanghai 200062, China; Email: wcm@fudan.edu.cn

Patrick L. Kinney — School of Public Health, Boston University, Boston 02118, Massachusetts, United States; Email: pkinney@bu.edu

Authors

Cheng He — Department of Environment Science and Engineering, Fudan University, Shanghai 200438, China; School of Public Health, Boston University, Boston 02118, Massachusetts, United States;  orcid.org/0000-0002-8470-0834

Junri Zhao — Department of Environment Science and Engineering, Fudan University, Shanghai 200438, China;  orcid.org/0000-0001-5464-8660

Yan Zhang — Department of Environment Science and Engineering and Big Data Institute for Carbon Emission and Environmental Pollution, Fudan University, Shanghai 200438, China; Shanghai Institute of Eco-Chongming (SIEC), Shanghai 200062, China;  orcid.org/0000-0003-3087-326X

Li He — Department of Environment Science and Engineering, Fudan University, Shanghai 200438, China

Youru Yao — School of Environment, Nanjing Normal University, Nanjing 210097, China

Complete contact information is available at:
<https://pubs.acs.org/10.1021/acs.est.0c03536>

Notes

The authors declare no competing financial interest.

ACKNOWLEDGMENTS

This work was funded by the National Key Research and Development Program of China (2016YFC0502706). C.H. gratefully acknowledged the support from the China Scholarship Council (201906100127).

REFERENCES

- (1) Zhou, L.; Dickinson, R. E.; Tian, Y.; Fang, J.; Li, Q.; Kaufmann, R. K.; Tucker, C. J.; Myneni, R. B. Evidence for a significant urbanization effect on climate in China. *Proc. Natl. Acad. Sci. U.S.A.* **2004**, *101*, 9540–9544.
- (2) Kalnay, E.; Cai, M. Impact of urbanization and land-use change on climate. *Nature* **2003**, *423*, 528.
- (3) Yin, P.; Chen, R.; Wang, L.; Liu, C.; Niu, Y.; Wang, W.; Jiang, Y.; Liu, Y.; Liu, J.; Qi, J.; You, J.; Zhou, M.; Kan, H. The added effects of heatwaves on cause-specific mortality: A nationwide analysis in 272 Chinese cities. *Environ. Int.* **2018**, *121*, 898–905.
- (4) He, C.; Ma, L.; Zhou, L.; Kan, H.; Zhang, Y.; Ma, W.; Chen, B. Exploring the mechanisms of heat wave vulnerability at the urban scale based on the application of big data and artificial societies. *Environ. Int.* **2019**, *127*, 573–583.
- (5) Li, Y.; Pizer, W. A.; Wu, L. Climate change and residential electricity consumption in the Yangtze River Delta, China. *Proc. Natl. Acad. Sci. U.S.A.* **2019**, *116*, 472–477.
- (6) Tao, W.; Liu, J.; Ban-Weiss, G. A.; Zhang, L.; Zhang, J.; Yi, K.; Tao, S. Potential impacts of urban land expansion on Asian airborne pollutant outflows. *J. Geophys. Res.: Atmos.* **2017**, *122*, 7646–7663.
- (7) Tao, W.; Liu, J.; Ban-Weiss, G.; Hauglustaine, D.; Zhang, L.; Zhang, Q.; Cheng, Y.; Yu, Y.; Tao, S. Effects of urban land expansion on the regional meteorology and air quality of eastern China. *Atmos. Chem. Phys.* **2015**, *15*, 8597.
- (8) Lin, L.; Luo, M.; Chan, T. O.; Ge, E.; Liu, X.; Zhao, Y.; Liao, W. Effects of urbanization on winter wind chill conditions over China. *Sci. Total Environ.* **2019**, *688*, 389–397.
- (9) Du, H.; Wang, D.; Wang, Y.; Zhao, X.; Qin, F.; Jiang, H.; Cai, Y. Influences of land cover types, meteorological conditions, anthropogenic heat and urban area on surface urban heat island in the Yangtze River Delta Urban Agglomeration. *Sci. Total Environ.* **2016**, *571*, 461–470.
- (10) Theeuwes, N. E.; Steeneveld, G. J.; Ronda, R. J.; Heusinkveld, B. G.; Van Hove, L. W. A.; Holtslag, A. A. M. Seasonal dependence of the urban heat island on the street canyon aspect ratio. *Q. J. R. Meteorol. Soc.* **2014**, *140*, 2197–2210.
- (11) Taha, H. Urban climates and heat islands: albedo, evapotranspiration, and anthropogenic heat. *Energy Build.* **1997**, *25*, 99–103.
- (12) Fan, H.; Sailor, D. Modeling the impacts of anthropogenic heating on the urban climate of Philadelphia: a comparison of implementations in two PBL schemes. *Atmos. Environ.* **2005**, *39*, 73–84.
- (13) Tan, Z.; Lau, K. K.-L.; Ng, E. Urban tree design approaches for mitigating daytime urban heat island effects in a high-density urban environment. *Energy Build.* **2016**, *114*, 265–274.
- (14) Kovats, R. S.; Hajat, S. Heat stress and public health: a critical review. *Annu. Rev. Public Health* **2008**, *29*, 41–55.
- (15) Li, D.; Bou-Zeid, E.; Oppenheimer, M. The effectiveness of cool and green roofs as urban heat island mitigation strategies. *Environ. Res. Lett.* **2014**, *9*, 055002.
- (16) Krayenhoff, E. S.; Moustaqi, M.; Broadbent, A. M.; Gupta, V.; Georgescu, M. Diurnal interaction between urban expansion, climate change and adaptation in US cities. *Nat. Clim. Change* **2018**, *8*, 1097.
- (17) Georgescu, M.; Morefield, P. E.; Bierwagen, B. G.; Weaver, C. P. Urban adaptation can roll back warming of emerging megapolitan regions. *Proc. Natl. Acad. Sci. U.S.A.* **2014**, *111*, 2909–2914.
- (18) Bowler, D. E.; Buyung-Ali, L.; Knight, T. M.; Pullin, A. S. Urban greening to cool towns and cities: A systematic review of the empirical evidence. *Landscape Urban Plann.* **2010**, *97*, 147–155.
- (19) Santamouris, M. Cooling the cities—a review of reflective and green roof mitigation technologies to fight heat island and improve comfort in urban environments. *Sol. Energy* **2014**, *103*, 682–703.
- (20) Sun, T.; Bou-Zeid, E.; Ni, G.-H. To irrigate or not to irrigate: analysis of green roof performance via a vertically-resolved hydrothermal model. *Build. Environ.* **2014**, *73*, 127–137.
- (21) Imran, H. M.; Kala, J.; Ng, A. W. M.; Muthukumaran, S. Effectiveness of green and cool roofs in mitigating urban heat island effects during a heatwave event in the city of Melbourne in southeast Australia. *J. Cleaner Prod.* **2018**, *197*, 393–405.
- (22) Kusaka, H.; Kimura, F. Thermal effects of urban canyon structure on the nocturnal heat island: Numerical experiment using a mesoscale model coupled with an urban canopy model. *J. Appl. Meteorol.* **2004**, *43*, 1899–1910.
- (23) Cao, M.; Rosado, P.; Lin, Z.; Levinson, R.; Millstein, D. Cool roofs in Guangzhou, China: outdoor air temperature reductions during heat waves and typical summer conditions. *Environ. Sci. Technol.* **2015**, *49*, 14672–14679.
- (24) Zhang, J.; Mohegh, A.; Li, Y.; Levinson, R.; Ban-Weiss, G. Systematic comparison of the influence of cool wall versus cool roof adoption on urban climate in the Los Angeles Basin. *Environ. Sci. Technol.* **2018**, *52*, 11188–11197.
- (25) Synnefa, A.; Saliari, M.; Santamouris, M. Experimental and numerical assessment of the impact of increased roof reflectance on a school building in Athens. *Energy Build.* **2012**, *55*, 7–15.
- (26) Pisello, A. L.; Cotana, F. The thermal effect of an innovative cool roof on residential buildings in Italy: Results from two years of continuous monitoring. *Energy Build.* **2014**, *69*, 154–164.
- (27) Mlawer, E. J.; Taubman, S. J.; Brown, P. D.; Iacono, M. J.; Clough, S. A. Radiative transfer for inhomogeneous atmospheres: RRTM, a validated correlated-k model for the longwave. *J. Geophys. Res.: Atmos.* **1997**, *102*, 16663–16682.
- (28) Dudhia, J. Numerical study of convection observed during the winter monsoon experiment using a mesoscale two-dimensional model. *J. Atmos. Sci.* **1989**, *46*, 3077–3107.

- (29) Lin, Y.-L.; Farley, R. D.; Orville, H. D. Bulk parameterization of the snow field in a cloud model. *J. Clim. Appl. Meteorol.* **1983**, *22*, 1065–1092.
- (30) Chen, F.; Dudhia, J. Coupling an advanced land surface–hydrology model with the Penn State–NCAR MMS modeling system. Part I: Model implementation and sensitivity. *Mon. Weather Rev.* **2001**, *129*, 569–585.
- (31) Lin, Y.-L.; Farley, R. D.; Orville, H. D. Bulk Parameterization of the Snow Field in a Cloud Model. *J. Clim. Appl. Meteorol.* **1983**, *22*, 1065–1092.
- (32) Mlawer, E. J.; Taubman, S. J.; Brown, P. D.; Iacono, M. J.; Clough, S. A. Radiative transfer for inhomogeneous atmosphere: RRTM, a validated correlated-k model for the longwave. *J. Geophys. Res.: Atmos.* **1997**, *102*, 16663–16682.
- (33) Kim, H.-J.; Wang, B. Sensitivity of the WRF model simulation of the East Asian summer monsoon in 1993 to shortwave radiation schemes and ozone absorption. *Asia Pac. J. Atmos. Sci.* **2011**, *47*, 167–180.
- (34) Chen, F.; Dudhia, J. Coupling an Advanced Land Surface Hydrology Model with the Penn State NCAR MMS Modeling System. Part I: Model Implementation and Sensitivity. *Mon. Weather Rev.* **2001**, *129*, 569–585.
- (35) Janjić, Z. I. The Step-Mountain Coordinate: Physical Package. *Mon. Weather Rev.* **1990**, *118*, 1429–1443.
- (36) Grell, G. A.; Dévényi, D. A generalized approach to parameterizing convection combining ensemble and data assimilation techniques. *Geophys. Res. Lett.* **2002**, *29*, 38.
- (37) Xie, M.; Liao, J.; Wang, T.; Zhu, K.; Zhuang, B.; Han, Y.; Li, M.; Li, S. Modeling of the anthropogenic heat flux and its effect on regional meteorology and air quality over the Yangtze River Delta region, China. *Atmos. Chem. Phys.* **2016**, *16*, 6071.
- (38) Xie, M.; Zhu, K.; Wang, T.; Feng, W.; Gao, D.; Li, M.; Li, S.; Zhuang, B.; Han, Y.; Chen, P.; Liao, J. Changes in regional meteorology induced by anthropogenic heat and their impacts on air quality in South China. *Atmos. Chem. Phys.* **2016**, *16*, 15011–15031.
- (39) Stewart, I. D.; Oke, T. R.; Krayenhoff, E. S. Evaluation of the ‘local climate zone’ scheme using temperature observations and model simulations. *Int. J. Climatol.* **2014**, *34*, 1062–1080.
- (40) Vahmani, P.; Jones, A.; Patricola, C. M. Interacting implications of climate change, population dynamics, and urban heat mitigation for future exposure to heat extremes. *Environ. Res. Lett.* **2019**, *14*, 084051.
- (41) Xie, M.; Liao, J.; Wang, T.; Zhu, K.; Zhuang, B.; Han, Y.; Li, M.; Li, S. Modeling of the anthropogenic heat flux and its effect on regional meteorology and air quality over the Yangtze River Delta region, China. *Atmos. Chem. Phys.* **2016**, *16*, 6071–6089.
- (42) He, C.; Zhou, L.; Yao, Y.; Ma, W.; Kinney, P. L. Estimating temporal-spatial effects of anthropogenic heat emissions upon the urban thermal environment in an urban agglomeration area in East China. *Sustain. Cities Soc.* **2020**, *57*, 102046.
- (43) Wang, Y.; Chen, L.; Song, Z.; Huang, Z.; Ge, E.; Lin, L.; Luo, M. Human-perceived temperature changes over South China: Long-term trends and urbanization effects. *Atmos. Res.* **2019**, *215*, 116–127.
- (44) Sun, R.; Wang, Y.; Chen, L. A distributed model for quantifying temporal-spatial patterns of anthropogenic heat based on energy consumption. *J. Cleaner Prod.* **2018**, *170*, 601–609.
- (45) Cao, M.; Rosado, P.; Lin, Z.; Levinson, R.; Millstein, D. Cool Roofs in Guangzhou, China: Outdoor Air Temperature Reductions during Heat Waves and Typical Summer Conditions. *Environ. Sci. Technol.* **2015**, *49*, 14672–14679.
- (46) Gaffin, S.; Rosenzweig, C.; Eichenbaum-Pikser, J.; Khanbilvardi, R.; Susca, T. *A Temperature and Seasonal Energy Analysis of Green, White, and Black Roofs*; Center for Climate Systems Research, Columbia University: New York, Technical Report, 2010.
- (47) Jandaghian, Z.; Touchaei, A. G.; Akbari, H. Sensitivity analysis of physical parameterizations in WRF for urban climate simulations and heat island mitigation in Montreal. *Urban Clim.* **2018**, *24*, 577–599.
- (48) Georgescu, M.; Morefield, P. E.; Bierwagen, B. G.; Weaver, C. P. Urban adaptation can roll back warming of emerging metropolitan regions. *Proc. Natl. Acad. Sci. U.S.A.* **2014**, *111*, 2909–2914.
- (49) Barozzi, B.; Pollastro, M. Assessment of the impact of cool roofs in temperate climates through a comparative experimental campaign in outdoor test cells. *Buildings* **2016**, *6*, 52.
- (50) Zhang, G.; He, B.-J.; Dewancker, B. J. The maintenance of prefabricated green roofs for preserving cooling performance: A field measurement in the subtropical city of Hangzhou, China. *Sustain. Cities Soc.* **2020**, *61*, 102314.
- (51) Zhang, J.; Li, Y.; Tao, W.; Liu, J.; Levinson, R.; Mohegh, A.; Ban-Weiss, G. Investigating the Urban Air Quality Effects of Cool Walls and Cool Roofs in Southern California. *Environ. Sci. Technol.* **2019**, *53*, 7532–7542.
- (52) Tang, M.; Zheng, X. Experimental study of the thermal performance of an extensive green roof on sunny summer days. *Appl. Energy* **2019**, *242*, 1010–1021.
- (53) Sproul, J.; Wan, M. P.; Mandel, B. H.; Rosenfeld, A. H. Economic comparison of white, green, and black flat roofs in the United States. *Energy Build.* **2014**, *71*, 20–27.